Cellular and Molecular Life Sciences (2021) 78:6709–6719
https://doi.org/10.1007/s00018-021-03940-5

ORIGINAL ARTICLE

Assessing eukaryotic initiation factor 4F subunit essentiality by CRISPR-induced gene ablation in the mouse

Patrick Sénéchal[1] · Francis Robert[1] · Regina Cencic[1] · Akiko Yanagiya[1,5] · Jennifer Chu[1,6] · Nahum Sonenberg[1,4] · Marilène Paquet[2] · Jerry Pelletier[1,3,4]

Received: 18 June 2021 / Revised: 31 August 2021 / Accepted: 10 September 2021 / Published online: 24 September 2021

Abstract

Eukaryotic initiation factor (eIF) 4F plays a central role in the ribosome recruitment phase of cap-dependent translation. This heterotrimeric complex consists of a cap binding subunit (eIF4E), a DEAD-box RNA helicase (eIF4A), and a large bridging protein (eIF4G). In mammalian cells, there are two genes encoding eIF4A (eIF4A1 and eIF4A2) and eIF4G (eIF4G1 and eIF4G3) paralogs that can assemble into eIF4F complexes. To query the essential nature of the eIF4F subunits in normal development, we used CRISPR/Cas9 to generate mouse strains with targeted ablation of each gene encoding the different eIF4F subunits. We find that *Eif4e*, *Eif4g1*, and *Eif4a1* are essential for viability in the mouse, whereas *Eif4g3* and *Eif4a2* are not. However, *Eif4g3* and *Eif4a2* do play essential roles in spermatogenesis. Crossing of these strains to the lymphoma-prone *Eμ-Myc* mouse model revealed that heterozygosity at the *Eif4e* or *Eif4a1* loci significantly delayed tumor onset. Lastly, tumors derived from $Eif4e^{\Delta 38\ fs/+}$/*Eμ-Myc* or $Eif4a1^{\Delta 5\ fs/+}$/*Eμ-Myc* mice show increased sensitivity to the chemotherapeutic agent doxorubicin, in vivo. Our study reveals that eIF4A2 and eIF4G3 play non-essential roles in gene expression regulation during embryogenesis; whereas reductions in eIF4E or eIF4A1 levels are protective against tumor development in a murine Myc-driven lymphoma setting.

Keywords GEMM · eIF4A2 · eIF4G3 · eIF4A1 · eIF4G1 · eIF4E · Translation

Introduction

Eukaryotic initiation factor (eIF) 4F is a cytoplasmic complex composed of three subunits: (i) eIF4E, a cap-binding protein which interacts with m^7G mRNA cap structures, (ii) eIF4G, which serves as a protein scaffold, and (iii) eIF4A, an RNA helicase necessary for remodeling mRNA templates to facilitate ribosome recruitment [1]. EIF4F, along with the RNA binding proteins eIF4B and eIF4H, are required to recruit ribosomes to mRNA templates. The role of eIF4F in regulating translation initiation is complex. Structural barriers (e. g., secondary structure, RNA bound proteins) within mRNA 5' leaders impair the process of translation initiation, cap recognition by eIF4F, and ribosome scanning [1]. Hence, different mRNAs harbor distinctive requirements for eIF4F-dependent ribosome recruitment—making eIF4F an mRNA discriminatory factor. As well, eIF4F assembly is regulated by the PI3K/AKT/mTOR pathway and there have been several lines of evidence implicating this complex in cancer initiation and maintenance, making it a promising target for anti-cancer therapies [2].

Patrick Sénéchal, Francis Robert and Regina Cencic shared co-authorship.

✉ Jerry Pelletier
jerry.pelletier@mcgill.ca

1 Department of Biochemistry, McGill University, Montreal, QC H3G 1Y6, Canada

2 Département de Pathologie et Microbiologie, Faculté de Médecine Vétérinaire, Université de Montréal, Saint-Hyacinthe, QC, Canada

3 Department of Oncology, McGill University, Montreal, QC H3A 1G5, Canada

4 Rosalind and Morris Goodman Cancer Research Center, McGill University, Montreal, QC H3A 1A3, Canada

5 Present Address: Cell Signal Unit, Okinawa Institute of Science and Technology, Okinawa 904-0495, Japan

6 Present Address: Department of Biology, Massachusetts Institute of Technology, Cambridge, MA 02138, USA

The mammalian genome encodes three different eIF4E paralogs, eIF4E1 (hereafter referred to as eIF4E), eIF4E2 (aka 4E-HP) and eIF4E3 [3]. Among these, eIF4E and eIF4E3 can interact with eIF4G to establish different eIF4F complexes [4]. However, eIF4E3 shows a restricted tissue expression profile, has significantly lower affinity for the cap than eIF4E, and is not essential in cell culture models as Hap1 cells harboring a frameshift (fs) mutation in the *EIF4E3* coding region are commercially available (https://horizondiscovery.com/en/engineered-cell-lines/products/human-hap1-knockout-cell-lines?nodeid=entrezgene-317649). On the other hand, *Eif4e1*$^{-/-}$ cells or mice have never been reported—consistent with the essential nature of *Eif4e1* [5].

Mammalian cells encode three eIF4G paralogs: eIF4G1 (aka eIF4GI), eIF4G2 (aka p97, Dap5, Nat1, eIF4GIII), and eIF4G3 (eIF4GII). eIF4G2 does not participate in eIF4F assembly as it lacks an eIF4E binding domain and instead, appears to play a more specialized role in cap-independent translation initiation, notably during stem cell differentiation and in ribosome recruitment via a cap-independent mechanism [6]. In contrast, eIF4G1 and eIF4G3 do interact with eIF4E and assemble into eIF4F. eIF4G1 and eIF4G3 share 48% amino acid identity, and although they show some differences regarding regulation by specific kinases or different sensitivities to viral and cellular proteases [7], recruitment of either protein to an mRNA template is sufficient to stimulate ribosome recruitment [4]. In humans, there are two additional proteins that share homology to the C-terminal domain of eIF4G proteins and that also interact with eIF3—known as eIF5-mimic protein (5MP1 and 5MP2) [8, 9]. They play an essential role in animal development and their over-expression is pro-oncogenic [10]. 5MP have been shown to reduce translation of *Eif4g2* mRNA by affecting start codon selection [11] and thus can impact eIF4G2-mediated translation.

There are two mammalian eIF4A paralogs involved in translation initiation, eIF4A1 and eIF4A2. Both share > 90% amino acid identity and can exchange into the eIF4F complex [12]. eIF4A1 is the most abundant initiation factor at ~ 3 copies per ribosome [13], with only a small fraction (~ 5%) present in the eIF4F complex—suggesting either that multiple molecules of eIF4A1 are required per initiation event and/or eIF4A1 also functions outside of the eIF4F complex [14]. In general, eIF4A1 is more abundantly expressed at the mRNA and protein level [13, 15]. The two *Eif4a* genes are differently regulated—with *Eif4a1*, but not *Eif4a2*, being under MYC transcriptional regulation. During growth arrest, eIF4A2 levels increase threefold whereas eIF4A1 levels are slightly reduced [16, 17]. As well, the two eIF4A paralogs show differential sensitivity to cleavage by foot-and-mouth disease virus 3C protease during viral infection [18]. The binding of eIF4A1 or eIF4A2 by RNA-bound eIF4G1 or eIF4G3 is sufficient to catalyze ribosome recruitment [4]. eIF4A1 is essential for cell survival, whereas eIF4A2 is not since it can be eliminated using CRISPR editing technology with no consequence on cell survival or proliferation [19]. What is difficult to reconcile with these aforementioned data are reports indicating that eIF4A2 is a suppressor of translation and mediates repression by microRNAs [20, 21].

The *Eμ-Myc* mouse is a powerful model that has been used to investigate the role of different translation initiation factors in tumorigenesis. The mice harbor a transgene in which an IgH enhancer has been juxtaposed next to c-Myc, a rearrangement similar to that found in Burkitt's lymphomas [22]. *Eμ-Myc* mice develop cancer with 100% penetrance and the consequences of genetic context on tumor development can be assessed by crossing *Eμ-Myc* mice to different genetically engineered mouse models and monitoring tumor development. Additionally, by isolating *Eμ-Myc* hematopoietic stem and progenitor cells (HSPCs) and introducing specific genetic lesions into these, followed by stem cell transplantation into normal recipients, one can assess the consequences of the introduced genetic changes on tumor onset [23, 24]. The effects of small molecules or biologicals on chemotherapeutic response of Myc-driven lymphomas can also be assessed in vivo in a syngeneic setting using this model. The consequences of eIF4E over-expression in this model has been assessed and found to cooperate with *Eμ-Myc* in accelerating lymphomagenesis [23, 24]. As well, eIF4E-overexpressing *Eμ-Myc* lymphomas are sensitive to shRNA- or small molecule mediated targeting of eIF4E and eIF4A, exhibiting a clear apoptotic response when combined with the front-line therapeutic, doxorubicin (DXR) [24–26].

Here, we asked whether all subunits of eIF4F play redundant roles in development and whether any are essential genes in the mouse. Secondarily, we also investigated what impact reductions in expression or gene loss of the eIF4F subunits has on Myc-driven lymphoma initiation. Lastly, we demonstrate a synthetic lethal relationship between *Eif4e* and *Eif4a1* gene dosage and DXR response in vivo.

Materials and methods

Transgenic mouse generation and genotyping

Mutations were produced on a C57BL/6 background using CRISPR/Cas9 editing technology. Single guide (sg) RNAs (shown in Fig. S1) were co-injected with purified, recombinant Cas9 protein into zygotes followed by re-implantation into pseudo-pregnant recipients. Upon weaning, mice were genotyped and those with PCR products showing a deletion upon gel analysis were directly analyzed by Sanger sequencing. Mice of the desired phenotype were then backcrossed to C57BL/6 wild-type mice. Primers for genotyping the

individual strains are: (i) *Eif4e* [eif4eko17744for: 5'CTCCTCCTGCAGGACGAGGAG3' and eif4erev: 5'TAGTACATGTCTTCACTGTCC3'], (ii) *Eif4a1* [m4a1ex5_3fwd: 5'AACCCCAGCCTTTGGATTTGG3' and 158-2Eif4a1ex5-2rev: 5'TCTCCGGTTAAGCATGTCCC3'], (iii) *Eif4a2* [4a2pcr2219-F: 5'GCACTGCTATATTGGCTTTG3' and 4a2seq2776-R: 5'GGACCATTAAGATTCACTAC3'], (iv) *Eif4g1* [meif4g1fwd: 5'CCAGCAGAACTGGGAGACTGTTGCATGTAGC3' and meif4g11drev: 5'TCGGGAGGCTGCACTGTAG3'], and (v) *Eif4g3* [4g3del171105_112298_F: 5'GTAGATAAGAATTCGAGATCC3' and 4g3seq112439-R: 5'CTCACTCTACTTACCTGAG3']. All mouse manipulations were performed at the McGill Integrated Core for Animal Modeling. All animal studies were approved by the McGill University Faculty of Medicine Animal Care Committee.

Western blotting

Western blots were performed on protein samples that had been prepared from spleens of mice of the indicated genotype. Upon harvesting, spleens were gently crushed between two microscope slides using the frosted portion of the slide. Cells were collected in PBS and filtered through a 40 µm nylon mesh. Cells were centrifuged at 1000xg for 5 min, and the pellet lysed in RIPA buffer (20 mM Tris–HCl [pH 7.6], 100 mM NaCl, 1 mM EDTA, 1 mM EGTA, 1% NP40, 0.5% sodium deoxycholate, 0.1% SDS, 10 mM NaF, 20 mM β-glycerophosphate, 1 mM PMSF, 4 µg/ml aprotinin, 2 µg/ml leupeptin, 2 µg/ml pepstatin, 1 mM DTT). Extracts were fractionated on a 10% SDS-PAGE and transferred to PVDF membranes (Bio-Rad). Antibodies used in this study were: α-eEF2 (Cell Signaling, 2332), α-eIF4E (Cell Signaling 9742), α-eIF4A1 (Abcam ab31217), α-eIF4A2 (Abcam ab31218), α-eIF4G1 [27], and α-eIF4G3 [28].

Tissue sectioning and staining

After harvesting, testes and epididymis were fixed in modified Davidson's fluid for 48 h, transferred to 70% ethanol and embedded in paraffin. Sections (4 µm) were deparaffinized in xylene, rehydrated, stained with hematoxylin and eosin or periodic acid-Schiff staining and mounted using Permount (Fisher, Canada). Sections were scanned on an Aperio ScanScope XT (Aperio Technologies, Vista, CA, USA).

Treatment studies

One million tumor cells were injected into the tail vein of 6–8 weeks old C57BL/6 females. When tumors were palpable, animals received one dose of DXR (10 mg/kg) intraperitoneally. Treatment response was monitored by palpation of lymph nodes every second day. Tumor-free survival is defined as the interval between DXR injection and the reemergence of tumor. Statistical evaluation of tumor-free survival was undertaken in the Kaplan–Meier format using Prism 8 and the log rank test.

Flow cytometry

Fresh lymphoma cells were harvested from tumor-bearing mice and resuspended in cold PBS. Erythrocytes were removed by lyzing in ACK buffer (150 mM NH_4Cl, 10 mM $KHCO_3$ and 0.1 mM EDTA) on ice for 10 min. Remaining cells were collected by centrifugation for 5 min at 1200×*g*, washed once in cold PBS and resuspended at 10^6 cells/ml in cold PBS + 2% fetal bovine serum (FBS). Cells (10^5) were added to prechilled tubes and gently mixed with 0.06 *u*g of antibodies followed by a 20 min incubation on ice in the dark. A control, unstained tube was also prepared for flow cytometry analysis. After incubation, 900 µl of cold PBS + 2% FBS was added, the cells spun down at 2500 × g for 5 min and flow cytometry analysis was conducted on a Guava EasyCyte HT (MilliporeSigma). Antibodies used were: CD19-PE (clone 6D5; Biolegend), B220-PE (clone RA3-6B2; BD Biosciences), IgM-PE (clone RMM-1, Biolegend), and CD3-PE (clone 17A2; BD Biosciences).

Statistical analysis

Results were calculated as mean ± standard deviation of the mean (Fig. 2). Sample size are indicated in figures or figure legends. Statistical analyses employed a one-way ANOVA with Tukey's multiple comparison test (Fig. 2) or the Kaplan–Meier format using the log-rank test for statistical significance (Fig. 4b). Statistical analysis was performed using GraphPad Prism v.8. A p value < 0.05 was taken as significant.

Results

Generation of KO mice

Genes encoding the eIF4F subunits: eIF4E, eIF4A1, eIF4A2, eIF4G1, and eIF4G3 were targeted for disruption using CRISPR/Cas9 (Figs. 1a and S1). The following mutant strains of mice were obtained and characterized.

(I) Mice harboring a 38 base pair (bp) deletion resulting in a frameshift mutation (fs) in *Eif4e*. Exon 6 of *Eif4e* was targeted for disruption, since a frameshift mutation within this area would disable cap-binding by producing a polypeptide lacking the downstream W102 amino acid critical for cap recognition (Figs. 1a, S1). A founder was obtained harboring a 38 bp fs expected to cause premature termination of translation within exon 6 (Fig S1a). Western blot analysis of

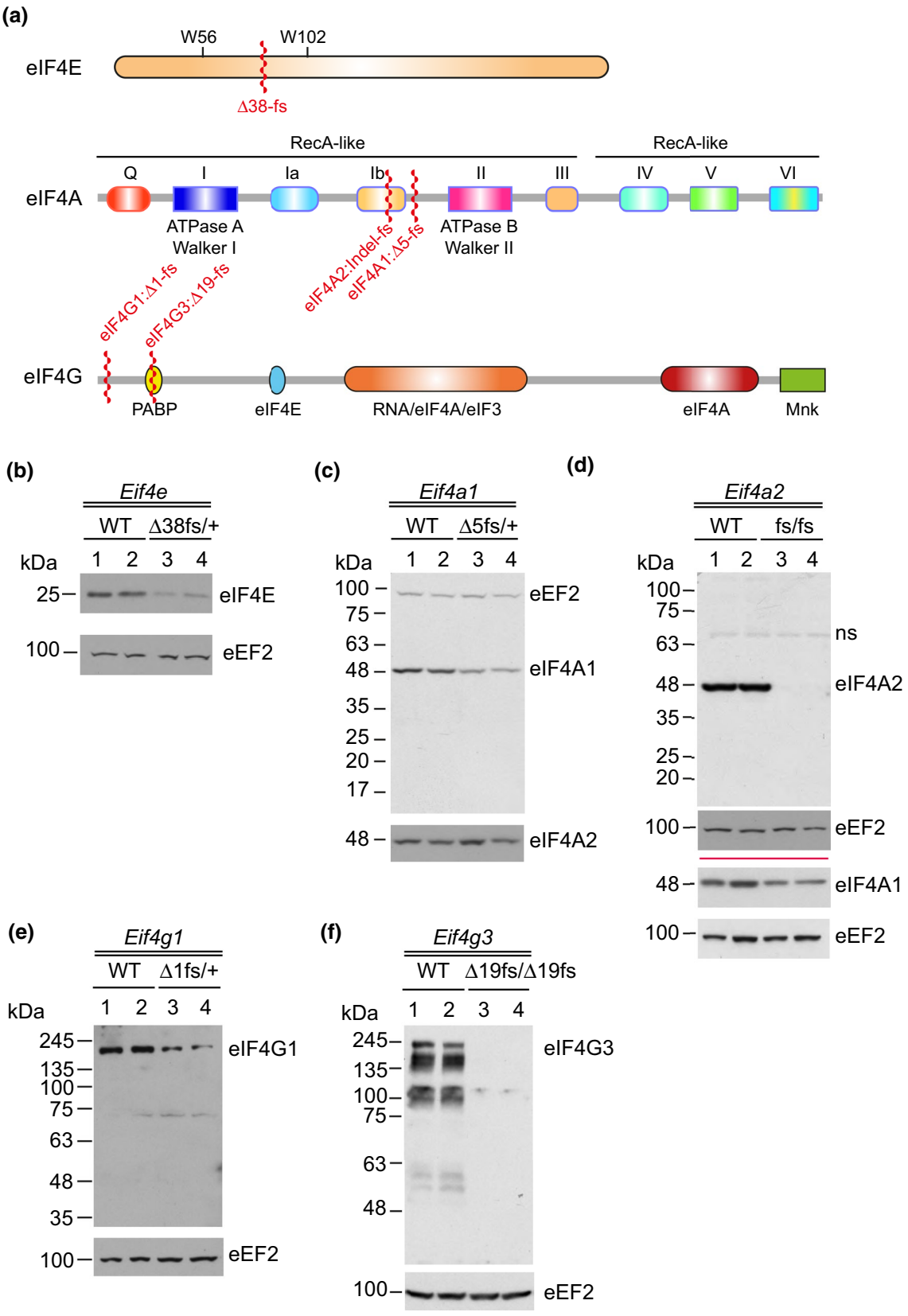
(a)
eIF4E
W56
W102
Δ38-fs
RecA-like
RecA-like
eIF4A
Q
I
Ia
Ib
II
III
IV
V
VI
ATPase A
Walker I
ATPase B
Walker II
eIF4A2:Indel-fs
eIF4A1:Δ5-fs
eIF4G1:Δ1-fs
eIF4G3:Δ19-fs
eIF4G
PABP
eIF4E
RNA/eIF4A/eIF3
eIF4A
Mnk
(b)
Eif4e
WT
Δ38fs/+
kDa
1 2 3 4
25
eIF4E
100
eEF2
(c)
Eif4a1
WT
Δ5fs/+
kDa
1 2 3 4
100
75
63
48
35
25
20
17
eEF2
eIF4A1
48
eIF4A2
(d)
Eif4a2
WT
fs/fs
kDa
1 2 3 4
100
75
63
48
35
25
20
ns
eIF4A2
100
eEF2
48
eIF4A1
100
eEF2
(e)
Eif4g1
WT
Δ1fs/+
kDa
1 2 3 4
245
135
100
75
63
48
35
eIF4G1
100
eEF2
(f)
Eif4g3
WT
Δ19fs/Δ19fs
kDa
1 2 3 4
245
135
100
75
63
48
eIF4G3
100
eEF2

◂**Fig. 1** Genetic targeting of eIF4F subunits. **a.** Schematic diagram illustrating location of CRISPR-Cas9 mediated mutagenesis of the indicated proteins—as denoted by red squiggles. Functional domains or amino acids critical to factor activity are indicated for reference. For eIF4E, W56 and W102 are essential for m^7G cap stacking. Δ, deletion; fs, frameshift. **b–f.** Western blots documenting reduction or loss of proteins from spleen of mice of the indicated genotypes. Proteins targeted by antibodies are indicated to the right of the blots. Samples collected from two wild-type (wt) and two mutant mice (genotype indicated above lanes) were processed and analyzed. The red horizontal line indicates two different sets of Western blots were used in the analysis, with one set above and the other below the red divider

spleen of *Eif4e*$^{\Delta 38\,fs/+}$ mice showed a ~ twofold reduction in protein levels, compared to levels present in wild-type (wt) littermates (Fig. 1b).

(II) Disruption of *Eif4a1* and *Eif4a2* coding potential by fs mutations. Exons 5 of *Eif4a1* and *Eif4a2* were selected for mutagenesis as fs mutations will produce truncated polypeptides lacking the critical C-terminal RecA-like domain (Fig. 1a). Founders with a 5 bp deletion resulting in a frameshift mutation in *Eif4a1* (*Eif4a1*$^{\Delta 5fs}$) or a more complex indel rearrangement in *Eif4a2* (*Eif4a2*^{fs}) were obtained (Fig. S1b, c). In the case of *Eif4a1*, splicing of exon 5 to exon 6 is predicted to lead to premature translation termination within exon 6. With respect to *Eif4a2*, a premature stop codon is generated within the indel region. Western blotting revealed a reduction in levels of eIF4A1 in *Eif4a1*$^{\Delta 5fs/+}$ mice and a complete loss of eIF4A2 in *Eif4a2*$^{fs/fs}$ mice, compared to wt littermates (Figs. 1c, d). There appears to be no compensatory increase in eIF4A2 or eIF4A1 protein levels in spleens from *Eif4a1*$^{\Delta 5fs/+}$ or *Eif4a2*^{fs} mice, respectively (Figs. 1c, d).

(III) Germline nonsense mutations in *Eif4g1* and *Eif4g3*. Exons 6 and 11 of *Eif4g1* and *Eif4g3*, respectively were targeted for disruption. Frameshift mutations arose in the *Eif4g1* (1 bp) and *Eif4g3* (19 bp) genes. Both mutations are predicted to lead to early termination of protein synthesis (Fig. S1d, e). Western blot analysis revealed a reduction in protein levels in spleen from *Eif4g1*$^{\Delta 1fs/+}$ mice and loss of expression in *Eif4g3*$^{\Delta 19fs/\Delta 19fs}$ mice, compared to wt littermates (Fig. 1e, f).

Eif4a2 and *Eif4g3* are not essential for development in the mouse

Crosses of wt mice to *Eif4e*$^{\Delta 38fs/+}$, *Eif4a1*$^{\Delta 5fs/+}$, *Eif4g1*$^{\Delta 1fs/+}$ heterozygotes showed deviation from the expected Mendelian inheritance with a lower than expected yield of heterozygote progeny, as determined by chi2 analysis (Table 1). These results indicate selection against animals with reduced dosage of *Eif4e, Eif4a1,* or *Eif4g1*. In contrast, crosses between wt and *Eif4a2*$^{fs/+}$ or *Eif4g3*$^{\Delta 19fs/+}$ mice showed segregation of the mutant alleles consistent with Mendelian inheritance (Table 1). Intercrosses of *Eif4e*$^{\Delta 38fs/+}$, *Eif4a1*$^{\Delta 5fs/+}$, or *Eif4g1*$^{\Delta 1fs/+}$ heterozygotes never yielded homozygous progeny attesting to the essential nature of these genes for viability and development. We make no conclusions as to the reason for the skewed ratios of wt and heterozygote offsprings obtained with *Eif4g1*$^{\Delta 1fs/+}$, compared to *Eif4a1*$^{\Delta 5fs/+}$, intercrosses since the number of breeding pairs that produced litters was too low ($N=4$) to be evaluated. Intercrosses between *Eif4a2*$^{fs/+}$ or *Eif4g3*$^{\Delta 19fs/+}$ mice produced progeny at the expected frequency indicating that neither *Eif4a2* nor *Eif4g3* are essential for mouse development.

We have noticed that at two months of age, *Eif4a2*$^{fs/fs}$ but not *Eif4g3*$^{\Delta 19fs/\Delta 19fs}$ mice, show lower body weights compared to heterozygotes or wild-type littermates. Here, both *Eif4a2*$^{fs/fs}$ female and male mice showed significant reductions in body weight compared to their heterozygote or wild-type counterparts (Fig. 2). We have not identified the underlying physiological basis for this but blood biochemistry analysis of *Eif4a2*$^{fs/fs}$ and *Eif4g3*$^{\Delta 19fs/\Delta 19fs}$ mice failed to uncover any overt metabolic perturbations (Table S1).

Male *Eif4a2*$^{fs/fs}$ and *Eif4g3*$^{\Delta 19fs/\Delta 19fs}$ mice are infertile

During the course of breeding and maintaining mice harboring the *Eif4a2*$^{fs/fs}$ or *Eif4g3*$^{\Delta 19fs/\Delta 19fs}$ alleles, we noticed that crosses of *Eif4a2*$^{fs/fs}$ or *Eif4g3*$^{\Delta 19fs/\Delta 19fs}$ males to C57BL/6 females never yielded offsprings. In contrast, crosses with *Eif4a2*$^{fs/fs}$ and *Eif4g3*$^{\Delta 19fs/\Delta 19fs}$ females to wild-type C57BL/6 males were productive (data not shown). We therefore analyzed spermatogenesis in *Eif4a2*$^{fs/fs}$ and *Eif4g3*$^{\Delta 19fs/\Delta 19fs}$ males for possible defects. Macroscopically, the testes of both genotypes showed moderate to severe bilateral atrophy when compared with wild-type controls (data not shown). Histopathologically, both genotypes demonstrated a moderate to severe diffuse atrophy of the seminiferous epithelium with patent efferent ducts and epididymis. Leydig cells from both strains appeared normal.

In testes from *Eif4a2*$^{fs/fs}$ mice, there was a late maturation arrest in spermatogenesis (Fig. 3a). Round spermatids were observed but did not mature into elongated spermatids. The arrest in spermatogenesis was in the early phases of spermiogenesis (spermatid maturation phases)—round spermatids prematurely exfoliated into the lumen before the elongation phase or aggregated in multinucleated symplasts. The efferent ducts were patent as evidenced by the large number of exfoliated round spermatids (Fig. 3b, visible in *Eif4a2*$^{fs/fs}$ testes) and symplasts distending the lumen of the epididymides (Fig. 3b). In sum, although stage XII meiosis events were observed in testes from *Eif4a2*$^{fs/fs}$ mice, there was a developmental arrest in the early stages of spermiogenesis; no mature elongated spermatids were present in any seminiferous tubules and this was associated with a deficiency in acrosomal maturation.

Table 1 Genotype distribution from the crosses of the indicated mouse strains

Crosses	*N*	Wild-type	Heterozygous	Homozygous	chi2	p value	Is deviation significant?
Eif4e(Δ38fs/+) × WT	33	120 (56%)	93 (44%)	N/A	3.423		no
Eif4e(Δ38fs/+) × Eif4e(Δ38fs/+)	6	9 (39%)	14 (61%)	0 (0%)	8.130	0.05 > p > 0.01	yes
Eif4a1(Δ5fs/+) × WT	55	215 (68%)	99 (32%)	N/A	42.853	< 0.01	yes
Eif4a1(Δ5fs/+) × Eif4a1(Δ5fs/+)	17	21 (38%)	34 (62%)	0 (0%)	19.109	< 0.01	yes
Eif4a2(fs/+) × WT	19	75 (52%)	70 (48%)	N/A	0.172		no
Eif4a2(fs/+) × Eif4a2(fs/+)	45	68 (23%)	135 (47%)	87 (30%)	3.869		no
Eif4g1(Δ1fs/+) × WT	38	132 (57%)	100 (43%)	N/A	4.414	0.05 > p > 0.01	yes
Eif4g1(Δ1fs/+) × Eif4g1(Δ1fs/+)	4	8(50%)	8(50%)	0 (0%)	8.000	0.05 > p > 0.01	yes
Eif4g3(Δ19fs/+) × WT	25	68 (47%)	78 (53%)	N/A	0.685		no
Eif4g3(Δ19fs/+) × Eif4g3(Δ19fs/+)	32	46 (25%)	88 (47%)	53 (28%)	1.171		no

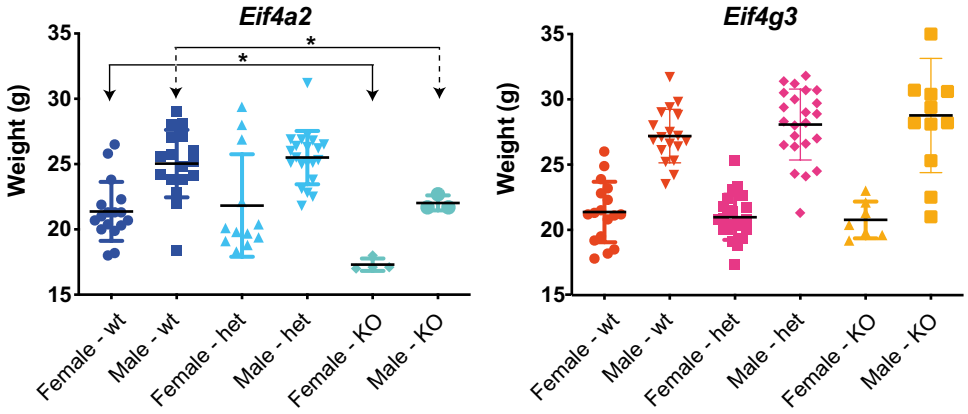

Fig. 2 Whole body weights of mice of the indicated genotypes taken at 10 weeks of age. Shown is the mean ± SD. Each point represents an independent mouse. *, $p < 0.001$

In testes from *Eif4g3*$^{\Delta 19fs/\Delta 19fs}$ mice, there appeared to be an early maturation arrest in spermatogenesis. Spermatogonia and spermatocytes were present but stage XII, as evidenced by meiosis, was absent leading to a diffuse absence of round and elongated spermatids (absence of spermiogenesis). There was severe atrophy of the seminiferous epithelium with large vacuoles in the Sertoli cells (Fig. 3a, red arrows). These developmental defects likely underlie the infertility of *Eif4a2*$^{fs/fs}$ and *Eif4g3*$^{\Delta 19fs/\Delta 19fs}$ males. Hence, eIF4A2 and eIF4G3 are essential for spermatogenesis in the mouse.

Dosage reduction of *Eif4e* or *Eif4a1* delays lymphomagenesis in the *Eμ-Myc* model

A reduction in *Eif4e* copy number suppresses in vitro transformation induced by Ras and Myc or Ras and E1A in murine embryonic fibroblasts (MEFs) and in vivo in KRas-driven lung tumors [5]. As well, experiments targeting different cancer types using eIF4A small molecule inhibitors, suppressing eIF4E expression using siRNAs, or dampening eIF4F activity through mTOR inhibition, have demonstrated that Myc-dependent tumors are quite responsive to eIF4F activity perturbation [26, 29–32]. We therefore wished to assess the consequences of *Eif4e*, *Eif4a1, Eif4a2*, *Eif4g1*, and *Eif4g3* gene dosage on MYC-induced tumor initiation.

To this end, we crossed our mutant strains to the *Eμ-Myc* mouse (Fig. 4a). This powerful model has been very informative for interrogating putative functional interactions between c-Myc and tumor suppressors or oncogenes [33]. We generated *Eμ-Myc* progeny harboring a single mutant allele of *Eif4e*, *Eif4a1*, or *Eif4g1* (since double mutants were not viable), as well as *Eμ-Myc* mice heterozygous or homozygous for *Eif4a2* or *Eif4g3* mutant alleles. Time to tumor onset was then documented (Fig. 4b–d). Only *Eif4e*$^{\Delta 38\ fs/+}$*/Eμ-Myc* and *Eif4a1*$^{\Delta 5\ fs/+}$*/Eμ-Myc* offsprings showed significant differences in tumor onset. We observed no significant differences in tumor onset rates of MYC-driven lymphomas in the absence of *Eif4a2* or *Eif4g3*, as well as upon reduction of *Eif4g1* allele levels.

Immuno-phenotyping indicated that *Eif4e*$^{\Delta 38\ fs/+}$*/Eμ-Myc* and *Eif4a1*$^{\Delta 5 fs/+}$*/Eμ-Myc* lymphomas were derived from a more mature progenitor (expressing CD19, B220, and IgM cell surface markers), whereas the sporadic *Eμ-Myc* lymphomas were derived from a less mature (CD19$^+$, B220$^+$) B cell progenitor (Fig. 4e). The absence of significant expression of

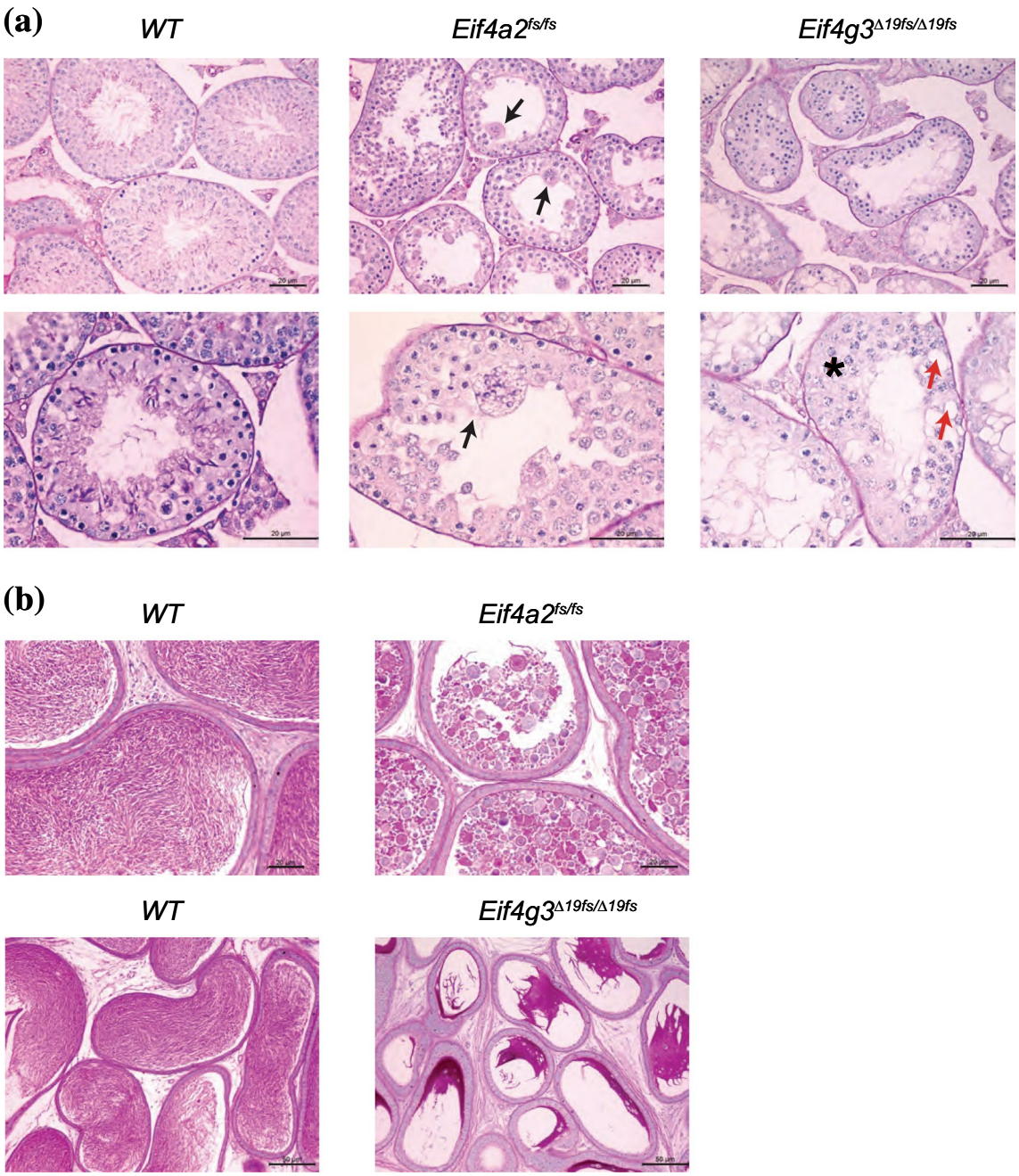

Fig. 3 Histological analysis of testes and epididymis from 2 months old *Eif4a2*$^{fs/fs}$ and *Eif4g3*$^{\Delta 19fs/\Delta 19fs}$ males. **a.** PAS-H stained testis sections. Spermatogonia, spermatocytes, round and elongated spermatids are present in wild-type testis. There is a complete lack of elongated spermatids in *Eif4a2*$^{fs/fs}$ and *Eif4g3*$^{\Delta 19fs/\Delta 19fs}$ males. The seminiferous epithelium is atrophied and the lumen is dilated. Black arrows denote the presence of multinucleated spermatids (symplasts). Red arrows indicate large vacuoles in Sertoli cells. Star highlights increased number of spermatocytes. Scale bar: 20 µm. **b.** PAS-H staining of the cauda epididymis from 2 months old *Eif4a2*$^{fs/fs}$ and *Eif4g3*$^{\Delta 19fs/\Delta 19fs}$ males. In wt mice, the lumen is filled with elongated spermatids (spermatozoa). In *Eif4g3*$^{\Delta 19fs/\Delta 19fs}$, the lumen is filled with protein rich fluid with few degenerated cells. In *Eif4a2*$^{fs/fs}$, the lumen of the cauda epididymis is filled with round spermatids and multinucleated cells prematurely exfoliated. Scale bar top: 20 µm; scale bar bottom: 50 µm

the T cell marker, CD3, is consistent with the B cell origin of these tumors (Fig. 4e).

Dosage reduction of *Eif4e* or *Eif4a1* is synthetic lethal with doxorubicin

Previous experiments using the *Eμ-Myc* model have shown

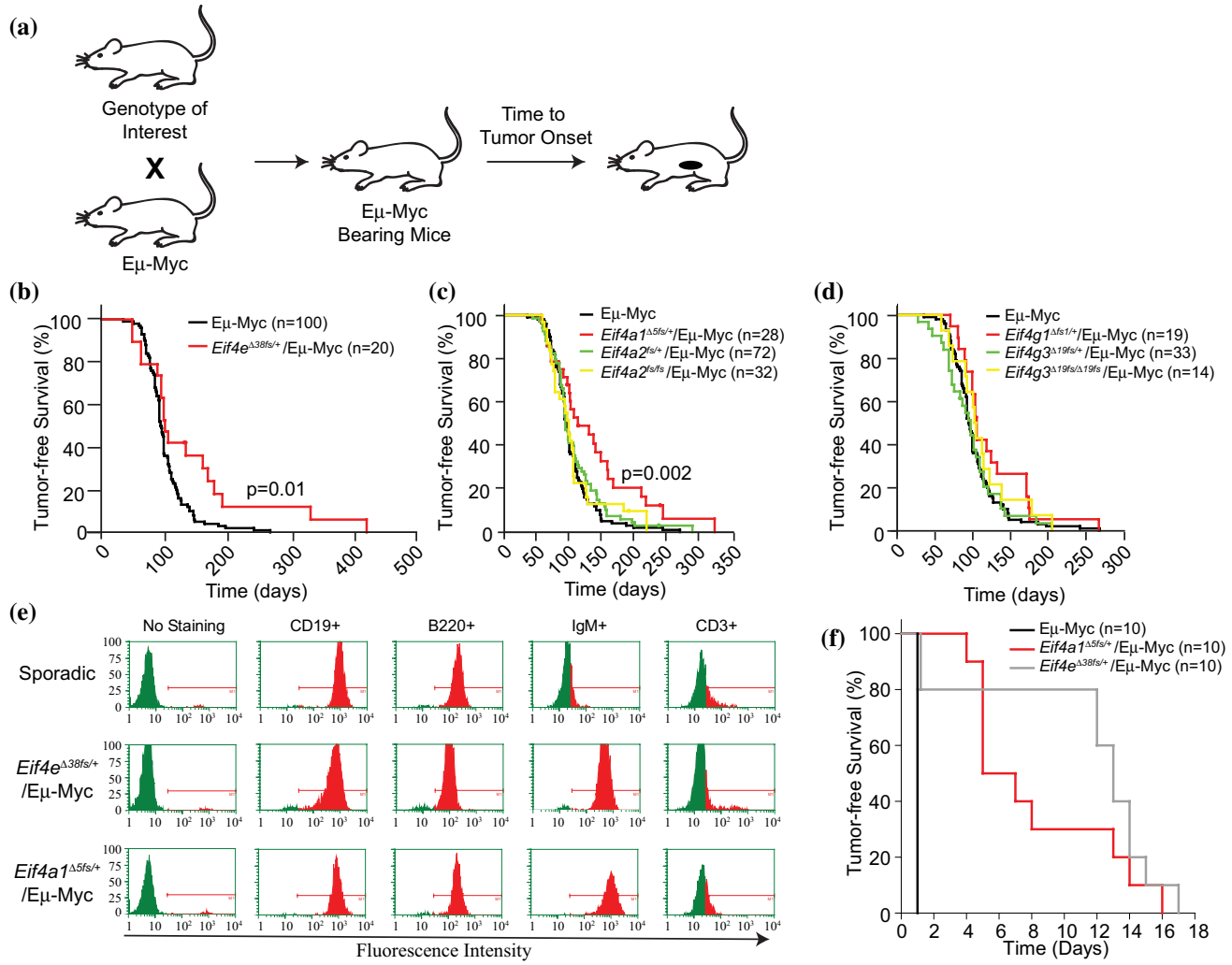

Fig. 4 Consequence of eIF4F subunit reduction or loss on *Eμ-Myc* driven lymphomagenesis. **a** Strategy used to monitor consequences of a given genotype on c-Myc induced tumor initiation. **b–d** Kaplan–Meier curves showing lymphoma tumor onset from mice of the indicated crosses. Note that the same *Eμ-Myc* reference curve is used in the panels and was obtained from monitoring 100 *Eμ-Myc* mice. The number of mice monitored in the individual experiments are indicated in parenthesis. **e.** Lineage marker expression in $Eif4e^{\Delta 38fs/+}$/*Eμ-Myc* and $Eif4a1^{\Delta 5fs/+}$/*Eμ-Myc* lymphomas. **f.** Reduced gene dosage of *Eif4e* and *Eif4a1* is synthetic lethal with DXR. Kaplan–Meier plot detailing time to relapse after DXR treatment of mice bearing lymphomas of the indicated genotype. Day 0 corresponds to the day of DXR treatment. $P < 0.00005$ for $Eif4e^{\Delta 38fs/+}$/*Eμ-Myc* and $Eif4a1^{\Delta 5fs/+}$/*Eμ-Myc* versus sporadic *Eμ-Myc* lymphomas

that suppression of eIF4E or eIF4A is capable of sensitizing *myr-Akt/Eμ-Myc*, $Tsc2^{-/+}$/*Eμ-Myc*, $Tsc1^{-/+}$/*Eμ-Myc*, and eIF4E-overexpression *Eμ-Myc* tumors to DXR [23, 24, 34]. Therefore, we wished to determine if $Eif4e^{\Delta 38fs/+}$/*Eμ-Myc* or $Eif4a1^{\Delta 5fs/+}$/*Eμ-Myc* lymphomas showed increased sensitivity to DXR. C57BL/6 mice harboring transplanted tumors were treated with a single bolus of DXR and monitored for tumor-free survival (Fig. 4f). Mice harboring sporadic *Eμ-Myc* lymphomas did not respond to DXR, as previously reported [23]. In contrast, a single bolus of DXR was sufficient to produce remission in both $Eif4e^{\Delta 38fs/+}$/*Eμ-Myc* and $Eif4a1^{\Delta 5fs/+}$/*Eμ-Myc* lymphoma-bearing mice.

Discussion

Eif4e, *Eif4a1*, and *Eif4g1*, but not *Eif4a2* and *Eif4g3*, are essential for development

In this study, we sought to define the essential nature of the eIF4F subunits by generating knockout models for all subunits. We found that *Eif4e*, *Eif4a1*, and *Eif4g1* are essential for mouse viability (Table 1). Haploinsufficiency of *Eif4e*, *Eif4a1*, and *Eif4g1* shows incomplete penetrance and partial lethality, consistent with their central role in regulating translation initiation. For *Eif4e*, our data is consistent with a study reported by Truitt et al. [5] in which *Eif4e* heterozygote

knockout mice (generated by insertional mutagenesis into exon 7) were found to be viable and had no distinguishing phenotype differences from their wt littermates. We have not analyzed the developmental stage at which loss of viability occurs in knockout mice null for *Eif4e*, *Eif4a1*, or *Eif4g1* but hypothesize that it will be very early in embryogenesis. Knockdown analysis of *EIF4E*, *EIF4A1*, and *EIF4G1* in 398 cancer cell lines (Project DRIVE) has shown all three subunits to be cell essential genes [35].

The commercial availability of *EIF4G3*-null Hap1 cells suggests, that consistent with our results in the mouse, these genes are not essential for survival (https://horizondiscovery.com). Both *EIF4A2* and *EIF4G3* have also been classified as non-essential genes following RNAi screens in 398 cancer cell lines [35]. As well, ablation of *Eif4a2* in NIH 3T3 cells is tolerated and does not impact on general translation or cellular proliferation [19]. Herein, we extend these results to report that neither *Eif4a2* nor *Eif4g3* are essential for viability and development in the mouse.

Eif4a2 and *Eif4g3* are required for normal spermatogenesis

Eif4a2 and *Eif4g3* play critical roles in spermatogenesis (Fig. 3). Regarding *Eif4g3*, a previously described mouse mutant, *repro8*, has been documented as harboring a missense mutation in *Eif4g3* and resembles the phenotype we described herein for $Eif4g3^{\Delta 19fs/\Delta 19fs}$ mice [36]. The *repro8* mutation arose in the last exon of *Eif4g3*, converts Ala1571 (NP_766291) to a proline, and leads to defective spermatogenesis due to an arrest in meiosis at the end of meiotic prophase [36]. A second *Eif4g3* mutant allele, leading to absence of the two last coding exons in the *Eif4g3* mRNA, failed to rescue the spermatogenesis defect when crossed into the *repro8* mice, providing genetic proof that mutation of this domain in *Eif4g3* is responsible for the described phenotype associated with the *repro8* mouse [36].

The C-terminus of eIF4G3 (and eIF4G1) mediates binding to the MNK1 and MNK2 kinases (*MKNK1* and *MKNK2*), which in turn phosphorylate eIF4G-bound eIF4E on Ser209 [37, 38]. Ablation of both *Mknk* genes in the mouse indicates that neither are essential for development [39]. It is thus unlikely that loss of Mnk1 and/or Mnk2 binding (and hence loss of eIF4E phosphorylation) is responsible for the defect on spermatogenesis per se observed with the $Eif4g3^{\Delta 19fs/\Delta 19fs}$ mouse, since double knockout $Mknk1^{-/-}Mknk2^{-/-}$ and $eIF4E^{S209A/S209A}$ knock-in mice do not show reproductive defects [39, 40]. Hence, the activity compromised by the A1571P mutation in the *repro8* mouse remains to be elucidated, but this mutant protein can still assemble into the eIF4F complex [41]; unlike in the $Eif4g3^{\Delta 19fs/\Delta 19fs}$ mice where there is no eIF4G3 present and thus no eIF4G3-containing eIF4F complex. It has been suggested that impaired translation of the mRNA encoding the heat-shock chaperone protein HSPA2—a protein required for activation of maturation-promoting factor (which in turn triggers entry into the mitotic and meiotic phases of the cell cycle) in $Eif4g3^{repro8}$ spermatocytes contributes to the impairment in spermatogenesis [36].

EIF4G1 is also expressed in germ cells during spermatogenesis, so the defect seen with *Eif4g3* mutant mice indicates a distinct role for eIF4G3 in gene expression regulation [41]. Whether this is translation related and/or due to a moonlighting function of eIF4G3 outside of translation is not known. The spermatogenesis defect present in $Eif4a2^{fs/fs}$ males that we have characterized arises at a later stage than what is observed in $Eif4g3^{\Delta 19fs/\Delta 19fs}$ mice (Fig. 3).

Dosage reduction of *Eif4e* or *Eif4a1* and Myc-driven tumor initiation

Haploinsufficiency for *Eif4e* has been previously shown to be compatible with normal development and protective towards tumor initiation [5]. Our results with $Eif4e^{\Delta 38fs/+}$/*Eμ-Myc* mice extend these findings in vivo to the lymphoma setting (Fig. 4b). Additionally, we find that haploinsufficiency for *Eif4a1*, but not *Eif4a2*, in the context of an *Eμ-Myc* allele, phenocopies the results obtained with $Eif4e^{\Delta 38fs/+}$/*Eμ-Myc* mice (Fig. 4c). Current effort is directed towards assessing if the affected translatomes in $Eif4e^{\Delta 38fs/+}$/*Eμ-Myc* and $Eif4a1^{\Delta 5fs/+}$/*Eμ-Myc* lymphomas are similar or different in nature. In the *Eμ-Myc* lymphoma setting, we did not see any significant impact on tumor burden arising due to insufficiency of *Eif4g1* or complete loss of *Eif4a2* or *Eif4g3*.

Given that the transforming potential of certain oncogenes are often revealed in specific contexts (e. g., cell types, expression levels) [42], we restrict our conclusions to the *Eμ-Myc* mouse model. In fact, over-expression of a cDNA encoding eIF4G1 in NIH3T3 cells has been shown to induce transformation in vitro [43] Over-expression of eIF4G1 is also a critical driver of tumorigenesis in inflammatory breast cancer, likely mediating its effects through re-programming translation to promote expression of IRES-containing mRNAs encoding proteins required for cell survival, growth, and tumor emboli [44, 45]. Thus, suppression of eIF4G1 expression has been shown to protect against tumor development.

We have previously shown that prophylactic treatment for 23 days of 4 week-old *Eμ-Myc* mice with silvestrol, a natural product that targets eIF4A, delays lymphoma onset [30]. This finding is consistent with our results herein with $Eif4e^{\Delta 38fs/+}$/*Eμ-Myc* and $Eif4a1^{\Delta 5fs/+}$/*Eμ-Myc* mice where reduced dosage levels of *Eif4e* and *Eif4a1* curtail Myc-dependent tumor initiation (Fig. 4). In the context of previous data demonstrating that small molecule-mediated inhibition of eIF4A leads to DXR re-sensitization in

mice bearing *Eμ-Myc*-derived lymphomas [25, 26, 46], we assessed if there was a synthetic lethal relationship between reductions in *Eif4e* and *Eif4a1* levels and DXR (Fig. 4f). The observed sensitivity of $Eif4e^{\Delta 38fs/+}$/*Eμ-Myc* and $Eif4a1^{\Delta 5fs/+}$/*Eμ-Myc* lymphomas to DXR is consistent with these previous findings.

In somatic cells, eIF4A1 is 11–19 times more abundant than eIF4E [13, 47, 48], making it difficult to reconcile how a reduction in *Eif4a1* gene dosage would affect eIF4F-mediated translation when eIF4E levels are still expected to remain limiting. These results may suggest that the total pool of eIF4A1 is not available for translation and is sequestered by negative regulatory binding partners, such as PDCD4 [49]. An allele reduction could then functionally limit the amounts of eIF4A1. As well, eIF4A1 may be geographically restricted in cells such that only a fraction of the total eIF4A1 pool is available for translation. Additionally, eIF4A1 has been found to restrict RNA-RNA interactions and limit their inherent ability to condense and participate in aggregations such as stress granules [14]. Stress granules appear to act as flexible regulators of gene expression in allowing cells to respond to evolving environment changes, among which may include cancer initiation programs and chemotherapy-induced stress [50]. Multiple molecules of eIF4A1 may also be required for each initiation round, in which case small reductions in eIF4A1 levels could impact on translation. The role of eIF4A1 in these events has yet to be explored.

In sum, eIF4A2 and eIF4G3 are largely dispensable for most developmental processes but in the context of spermatogenesis play essential roles. We find no evidence for redundancy between *Eif4a1* and *Eif4a2* nor between *Eif4g1* and *Eif4g3* since neither *Eif4a2* nor *Eif4g3* could rescue the lethality associate with complete loss of *Eif4a1* or *Eif4g1*, respectively. We find reductions in eIF4E or eIF4A1 levels to be protective in a murine MYC-driven lymphoma model.

Supplementary Information The online version contains supplementary material available at https://doi.org/10.1007/s00018-021-03940-5.

Author contributions PS: methodology, reviewing and editing, data curation. FR: methodology, reviewing and editing, data curation. RC: methodology, reviewing and editing, data curation. AY: methodology, reviewing and editing. JC: methodology, reviewing and editing. NS: resources, supervision, reviewing and editing, funding acquisition. MP: methodology, reviewing and editing. JP: conceptualization, methodology, writing—original draft, writing—reviewing and editing, visualization, supervision, funding acquisition.

Funding This study was supported by funding to JP (Canadian Institutes of Health Research [#FDN-148366]).

Data availability The datasets generated during and/or analyzed during the current study are available from the corresponding author on reasonable request.

Code availability Not applicable.

Declarations

Conflict of interest The authors declare no conflict of interest.

Ethical approval All mouse manipulations were performed at the McGill Integrated Core for Animal Modeling. All animal studies were approved by the McGill University Faculty of Medicine Animal Care Committee.

Consent to participate Not applicable.

Consent for publication Not applicable.

References

1. Pelletier J, Sonenberg N (2019) The organizing principles of eukaryotic ribosome recruitment. Annu Rev Biochem 88:307–335
2. Robichaud N, Sonenberg N, Ruggero D, Schneider RJ (2019) Translational control in cancer. Cold Spring Harb Perspect Biol 11:a032896
3. Joshi B, Cameron A, Jagus R (2004) Characterization of mammalian eIF4E-family members. Eur J Biochem 271:2189–2203
4. Robert F, Cencic R, Cai R, Schmeing TM, Pelletier J (2020) RNA-tethering assay and eIF4G:eIF4A obligate dimer design uncovers multiple eIF4F functional complexes. Nucl Acids Res 48:8562–8575
5. Truitt ML et al (2015) Differential requirements for eIF4E dose in normal development and cancer. Cell 162:59–71
6. Sugiyama H et al (2017) Nat1 promotes translation of specific proteins that induce differentiation of mouse embryonic stem cells. Proc Natl Acad Sci USA 114:340–345
7. Castello A, Alvarez E, Carrasco L (2011) The multifaceted poliovirus 2A protease: regulation of gene expression by picornavirus proteases. J Biomed Biotechnol. https://doi.org/10.1155/2011/369648
8. Singh CR et al (2011) Mechanisms of translational regulation by a human eIF5-mimic protein. Nucl Acids Res 39:8314–8328
9. Hiraishi H et al (2014) Essential role of eIF5-mimic protein in animal development is linked to control of ATF4 expression. Nucl Acids Res 42:10321–10330
10. Kozel C et al (2016) Overexpression of eIF5 or its protein mimic 5MP perturbs eIF2 function and induces ATF4 translation through delayed re-initiation. Nucl Acids Res 44:8704–8713
11. Tang L et al (2017) Competition between translation initiation factor eIF5 and its mimic protein 5MP determines non-AUG initiation rate genome-wide. Nucl Acids Res 45:11941–11953
12. Yoder-Hill J, Pause A, Sonenberg N, Merrick WC (1993) The p46 subunit of eukaryotic initiation factor (eIF)-4F exchanges with eIF-4A. J Biol Chem 268:5566–5573
13. Kulak NA, Pichler G, Paron I, Nagaraj N, Mann M (2014) Minimal, encapsulated proteomic-sample processing applied to copy-number estimation in eukaryotic cells. Nat Methods 11:319–324
14. Tauber D, Tauber G, Khong A, Van Treeck B, Pelletier J, Parker R (2020) Modulation of RNA condensation by the DEAD-box protein eIF4A. Cell 180:411-426e16
15. Nielsen PJ, Trachsel H (1988) The mouse protein synthesis initiation factor 4A gene family includes two related functional genes which are differentially expressed. EMBO J 7:2097–2105
16. Williams-Hill DM, Duncan RF, Nielsen PJ, Tahara SM (1997) Differential expression of the murine eukaryotic translation

initiation factor isogenes eIF4A(I) and eIF4A(II) is dependent upon cellular growth status. Arch Biochem Biophys 338:111–120
17. Lin CJ, Cencic R, Mills JR, Robert F, Pelletier J (2008) c-Myc and eIF4F are components of a feedforward loop that links transcription and translation. Cancer Res 68:5326–5334
18. Li W, Ross-Smith N, Proud CG, Belsham GJ (2001) Cleavage of translation initiation factor 4AI (eIF4AI) but not eIF4AII by foot-and-mouth disease virus 3C protease: identification of the eIF4AI cleavage site. FEBS Lett 507:1–5
19. Galicia-Vazquez G, Chu J, Pelletier J (2015) eIF4AII is dispensable for miRNA-mediated gene silencing. RNA 21:1826–1833
20. Wilczynska A et al (2019) eIF4A2 drives repression of translation at initiation by Ccr4-Not through purine-rich motifs in the 5'UTR. Genome Biol 20:262
21. Meijer HA et al (2013) Translational repression and eIF4A2 activity are critical for microRNA-mediated gene regulation. Science 340:82–85
22. Adams JM, Harris AW, Pinkert CA, Corcoran LM, Alexander WS, Cory S, Palmiter RD, Brinster RL (1985) The c-myc oncogene driven by immunoglobulin enhancers induces lymphoid malignancy in transgenic mice. Nature 318:533–538
23. Wendel HG et al (2004) Survival signalling by Akt and eIF4E in oncogenesis and cancer therapy. Nature 428:332–337
24. Wendel HG et al (2007) Dissecting eIF4E action in tumorigenesis. Genes Dev 21:3232–3237
25. Bordeleau ME et al (2008) Therapeutic suppression of translation initiation modulates chemosensitivity in a mouse lymphoma model. J Clin Invest 118:2651–2660
26. Cencic R et al (2013) Modifying chemotherapy response by targeted inhibition of eukaryotic initiation factor 4A. Blood Cancer J 3:e128
27. Morino S, Imataka H, Svitkin YV, Pestova TV, Sonenberg N (2000) Eukaryotic translation initiation factor 4E (eIF4E) binding site and the middle one-third of eIF4GI constitute the core domain for cap-dependent translation, and the C-terminal one-third functions as a modulatory region. Mol Cell Biol 20:468–477
28. Goldstaub D, Gradi A, Bercovitch Z, Grosmann Z, Nophar Y, Luria S, Sonenberg N, Kahana C (2000) Poliovirus 2A protease induces apoptotic cell death. Mol Cell Biol 20:1271–1277
29. Robert F et al (2014) Translation initiation factor eIF4F modifies the dexamethasone response in multiple myeloma. Proc Natl Acad Sci USA 111:13421–13426
30. Lin CJ, Nasr Z, Premsrirut PK, Porco JA Jr, Hippo Y, Lowe SW, Pelletier J (2012) Targeting synthetic lethal interactions between Myc and the eIF4F complex impedes Tumorigenesis. Cell Rep 1:325–333
31. Graff JR et al (2007) Therapeutic suppression of translation initiation factor eIF4E expression reduces tumor growth without toxicity. J Clin Invest 117:2638–2648
32. Pourdehnad M, Truitt ML, Siddiqi IN, Ducker GS, Shokat KM, Ruggero D (2013) Myc and mTOR converge on a common node in protein synthesis control that confers synthetic lethality in Myc-driven cancers. Proc Natl Acad Sci USA 110:11988–11993
33. Strasser A, Harris AW, Bath ML, Cory S (1990) Novel primitive lymphoid tumours induced in transgenic mice by cooperation between myc and bcl-2. Nature 348:331–333
34. Mills JR et al (2008) mTORC1 promotes survival through translational control of Mcl-1. Proc Natl Acad Sci USA 105:10853–10858
35. McDonald ER 3rd et al (2017) Project DRIVE: a compendium of cancer dependencies and synthetic lethal relationships uncovered by large-scale, deep RNAi screening. Cell 170:577-592e10
36. Sun F, Palmer K, Handel MA (2010) Mutation of Eif4g3, encoding a eukaryotic translation initiation factor, causes male infertility and meiotic arrest of mouse spermatocytes. Development 137:1699–1707
37. Pyronnet S, Imataka H, Gingras AC, Fukunaga R, Hunter T, Sonenberg N (1999) Human eukaryotic translation initiation factor 4G (eIF4G) recruits mnk1 to phosphorylate eIF4E. EMBO J 18:270–279
38. Waskiewicz AJ, Johnson JC, Penn B, Mahalingam M, Kimball SR, Cooper JA (1999) Phosphorylation of the cap-binding protein eukaryotic translation initiation factor 4E by protein kinase Mnk1 in vivo. Mol Cell Biol 19:1871–1880
39. Ueda T, Watanabe-Fukunaga R, Fukuyama H, Nagata S, Fukunaga R (2004) Mnk2 and Mnk1 are essential for constitutive and inducible phosphorylation of eukaryotic initiation factor 4E but not for cell growth or development. Mol Cell Biol 24:6539–6549
40. Furic L et al (2010) eIF4E phosphorylation promotes tumorigenesis and is associated with prostate cancer progression. Proc Natl Acad Sci USA 107:14134–14139
41. Hu J, Sun F, Handel MA (2018) Nuclear localization of EIF4G3 suggests a role for the XY body in translational regulation during spermatogenesis in mice. Biol Reprod 98:102–114
42. Gidekel Friedlander SY et al (2009) Context-dependent transformation of adult pancreatic cells by oncogenic K-Ras. Cancer Cell 16:379–389
43. Fukuchi-Shimogori T, Ishii I, Kashiwagi K, Mashiba H, Ekimoto H, Igarashi K (1997) Malignant transformation by overproduction of translation initiation factor eIF4G. Cancer Res 57:5041–5044
44. Silvera D, Schneider RJ (2009) Inflammatory breast cancer cells are constitutively adapted to hypoxia. Cell Cycle 8:3091–3096
45. Silvera D, Formenti SC, Schneider RJ (2010) Translational control in cancer. Nat Rev Cancer 10:254–266
46. Rodrigo CM, Cencic R, Roche SP, Pelletier J, Porco JA (2012) Synthesis of rocaglamide hydroxamates and related compounds as eukaryotic translation inhibitors: synthetic and biological studies. J Med Chem 55:558–562
47. Duncan R, Milburn SC, Hershey JW (1987) Regulated phosphorylation and low abundance of HeLa cell initiation factor eIF-4F suggest a role in translational control. Heat shock effects on eIF-4F. J Biol Chem 262:380–388
48. Galicia-Vazquez G, Cencic R, Robert F, Agenor AQ, Pelletier J (2012) A cellular response linking eIF4AI activity to eIF4AII transcription. RNA 18:1373–1384
49. Yang HS et al (2003) The transformation suppressor Pdcd4 is a novel eukaryotic translation initiation factor 4A binding protein that inhibits translation. Mol Cell Biol 23:26–37
50. Anderson P, Kedersha N, Ivanov P (2015) Stress granules, P-bodies and cancer. Biochim Biophys Acta 1849:861–870